

Slew Maneuver Control of Flexible Spacecraft

Süleyman Altınışık and Ozan Tekinalp***

**Doctoral Student, Department of Aerospace Engineering*

Middle East Technical University, Ankara, 06800, Turkey, e174673@metu.edu.tr

*** Professor, Department of Aerospace Engineering*

Middle East Technical University, Ankara, 06800, Turkey, tekinalp@metu.edu.tr

Abstract

Nonlinear slew maneuver algorithms for flexible spacecraft are developed. The attitude tracking algorithm that uses quaternion parametrization and follows the prescribed time dependent attitude trajectory incorporating the derivative of the desired attitude is employed. Nonlinear tracking feedback control algorithms that includes piezoelectric actuators and modal sensors are also developed. Through simulations, the effectiveness of the tracking attitude control algorithm is demonstrated. Also demonstrated is the effectiveness of the tracking controller utilizing piezoelectric actuators modal sensors in damping out vibration energy.

1. Introduction

Next generation spacecraft will need massive amounts of electrical energy to accomplish its missions such as interplanetary missions [1]. Earth observation missions that those employ synthetic aperture radar also require too much power for its operation. Such as energy will come from huge solar panels to absorb enough sunlight. These panels should also be lightweight. This requirement can also be satisfied by producing satellites with a large solar panels. Beside solar panels interplanetary spacecraft will also require large antennas to communicate with Earth from far away distances.

To increase service life and reduce the launch cost, most of the modern satellite often employ large-scale and lightly damped structures for antennas and solar arrays. This design restriction has become a major challenge recently due to flexibility and resulting excessive vibration on spacecraft. These effects may cause many problems in the satellite. Structural failure may be observed due to vibration, or satellite normal operations may be interrupted because of the undesired motion of flexible appendages. These flexible satellites need to carry out large slew maneuvers with high pointing precision and stability to perform complex space missions such as Earth observation and space monitoring. Designing an attitude control algorithm that compensates for this vibration and flexibility effects on satellite, is a challenging task.

Among the active control schemes, piezoelectric actuators have attracted interest as a solution for the attenuation of flexible spacecraft oscillations ([2], [3], [4]). There are some studies on these devices that demonstrate its effectiveness to damp out vibration experimentally ([5], [6]). Moreover, these devices are lightweight and they also have low power consumption. Their basic action is to increase the stiffness and the internal damping of the system.

On the other hand smooth slew maneuvers are needed not to violently excite the structural modes of the spacecraft. The well-known quaternion error feedback algorithm [7], is not quite suitable for smooth attitude maneuvers with precise pointing. Recently, new algorithms that uses the *to-go* quaternion propagation where the derivative of the desired attitude quaternion is employed are presented ([8], [9]). Given a smooth time dependent attitude trajectory, the algorithm is shown to accomplish tracking control successfully. This manuscript proposes using both piezo actuators and the recently developed quaternion based feedback algorithm to carry out smooth attitude maneuvers.

In the next section, the mathematical models of the flexible spacecraft, and the *to-go* attitude derivation that takes the desired attitude into account is presented. The attitude control algorithms are given next. It is followed by a parametric study that considers various effects such as utilization of piezo sensors and actuators. Finally some concluding remarks are given.

2. Mathematical Modeling

2.1 Quaternion Parametrization

Quaternion parametrization is used for attitude propagation. It is based on the *to-go* quaternion formulation that takes the time dependent desired attitude trajectory into account. The derivative of the to-go quaternion is derived. Let define the quaternion associated with the desired attitude using d , and current attitude using q , then the to-go attitude t may be written as ([8], [9]),

$$d = q \otimes t \text{ or } t = q^{-1} \otimes d \quad (1)$$

where, q^{-1} denotes the inverse or conjugate quaternion, since only unit quaternions are considered. In the above definition, the to-go quaternion obtained is the conjugate of the error quaternion used in the literature [7].

In vector matrix form,

$$\begin{Bmatrix} t_1 \\ t_2 \\ t_3 \\ t_4 \end{Bmatrix} = \begin{bmatrix} -d_4 & -d_3 & d_2 & d_1 \\ d_3 & -d_4 & -d_1 & d_2 \\ -d_2 & d_1 & -d_4 & d_3 \\ d_1 & d_2 & d_3 & d_4 \end{bmatrix} \begin{Bmatrix} q_1 \\ q_2 \\ q_3 \\ q_4 \end{Bmatrix} \quad (2)$$

or,

$$\begin{Bmatrix} \mathbf{t} \\ t_4 \end{Bmatrix} = \mathbf{D} \begin{Bmatrix} \mathbf{q} \\ q_4 \end{Bmatrix} \quad (3)$$

Using the chain rule, the derivative of the *to-go* quaternion may be obtained ([8], [9]),

$$\begin{Bmatrix} \dot{\mathbf{t}} \\ \dot{t}_4 \end{Bmatrix} = \dot{\mathbf{D}} \begin{Bmatrix} \mathbf{q} \\ q_4 \end{Bmatrix} + \mathbf{D} \begin{Bmatrix} \dot{\mathbf{q}} \\ \dot{q}_4 \end{Bmatrix} \quad (4)$$

In general, the desired final attitude is fixed. However, for tracking control, the time dependent feature of the desired attitude maybe taken into account. Remembering that the derivative of an attitude quaternion is given as (i.e., [7])

$$\begin{Bmatrix} \dot{\mathbf{q}} \\ \dot{q}_4 \end{Bmatrix} = \frac{1}{2} \begin{bmatrix} -\omega^x & \omega \\ -\omega^T & 0 \end{bmatrix} \begin{Bmatrix} \mathbf{q} \\ q_4 \end{Bmatrix} = \frac{1}{2} \boldsymbol{\Omega} \begin{Bmatrix} \mathbf{q} \\ q_4 \end{Bmatrix} \quad (5)$$

Equation (5) may be rewritten as [8],

$$\begin{Bmatrix} \dot{\mathbf{t}} \\ \dot{t}_4 \end{Bmatrix} = \dot{\mathbf{D}} \begin{Bmatrix} \mathbf{q} \\ q_4 \end{Bmatrix} + \frac{1}{2} \mathbf{D} \boldsymbol{\Omega} \begin{Bmatrix} \mathbf{q} \\ q_4 \end{Bmatrix} \quad (6)$$

Define the parameter,

$$\mathbf{D}_1 = \begin{bmatrix} -d_4 & d_3 & -d_2 & d_1 \\ -d_3 & -d_4 & d_1 & d_2 \\ d_2 & -d_1 & -d_4 & d_3 \\ d_1 & d_2 & d_3 & d_4 \end{bmatrix} \quad (7)$$

and

$$\begin{Bmatrix} \dot{\mathbf{t}} \\ \dot{t}_4 \end{Bmatrix} = \left[\dot{\mathbf{D}} \mathbf{D}_1 + \frac{1}{2} \mathbf{D} \boldsymbol{\Omega} \mathbf{D}_1 \right] \begin{Bmatrix} \mathbf{t} \\ t_4 \end{Bmatrix} \quad (8)$$

After some simplifications □[8], the following is obtained:

$$\begin{Bmatrix} \dot{\mathbf{t}} \\ \dot{t}_4 \end{Bmatrix} = \left[\begin{bmatrix} -s^x & \mathbf{s} \\ -s^T & 0 \end{bmatrix} + \mathbf{I} s_4 + \frac{1}{2} \begin{bmatrix} -\boldsymbol{\omega}^x & -\boldsymbol{\omega} \\ \boldsymbol{\omega}^T & 0 \end{bmatrix} \right] \begin{Bmatrix} \mathbf{t} \\ t_4 \end{Bmatrix} \quad (9)$$

where,

$$\mathbf{s} = \begin{Bmatrix} \dot{d}_1 d_4 + \dot{d}_2 d_3 - \dot{d}_3 d_2 - \dot{d}_4 d_1 \\ -\dot{d}_1 d_3 + \dot{d}_2 d_4 + \dot{d}_3 d_1 - \dot{d}_4 d_2 \\ \dot{d}_1 d_2 - \dot{d}_2 d_1 + \dot{d}_3 d_4 - \dot{d}_4 d_3 \end{Bmatrix}, \text{ and } s_4 = \dot{d}_1 d_1 + \dot{d}_2 d_2 + \dot{d}_3 d_3 + \dot{d}_4 d_4 = 0 \quad (10)$$

and \mathbf{I} is an identity matrix of proper dimension. It may easily be observed that $s_4 = 0$, and derivative of the to-go quaternion may be written as (□[8], □[9]),

$$\begin{aligned} \dot{\mathbf{t}} &= -\left(s^x + \frac{1}{2} \boldsymbol{\omega}^x\right) \mathbf{t} + \left(s - \frac{1}{2} \boldsymbol{\omega}\right) t_4 \\ \dot{t}_4 &= \left(-s^T + \frac{1}{2} \boldsymbol{\omega}^T\right) \mathbf{t} \end{aligned} \quad (11)$$

The above *to-go* quaternion attitude propagation algorithm takes the derivative of the desired trajectory into account, resulting in the actual attitude propagation, to track the time dependent desired attitude. If the desired attitude is fixed, then the usual *to-go* quaternion propagation algorithm is recovered:

$$\begin{Bmatrix} \dot{\mathbf{t}} \\ \dot{t}_4 \end{Bmatrix} = \frac{1}{2} \begin{bmatrix} -\omega^x & -\omega \\ \omega^T & 0 \end{bmatrix} \begin{Bmatrix} \mathbf{t} \\ t_4 \end{Bmatrix} \quad (12)$$

2.2 Mathematical Model of Flexible Spacecraft

Generalized flexible spacecraft dynamic may be obtained as follows [10]:

$$\begin{aligned} J\dot{\omega} + H^T\ddot{\eta} &= u \\ \ddot{\eta} + C\dot{\eta} + K\eta &= -H\dot{\omega} \end{aligned} \quad (13)$$

In the above equation, J is the inertia matrix of whole undeformed structure which is symmetric positive definite, η is the vector of modal coordinates of flexible modes being considered, H defines the coupling matrix between flexible and rigid dynamics, ω is the angular velocity of the main body and finally u is the control torque to be used. If there are distributed actuators such as piezoelectric actuators, then the equation takes the following form [10]:

$$\begin{aligned} J\dot{\omega} + H^T\ddot{\eta} &= u \\ \ddot{\eta} + C\dot{\eta} + K\eta &= -H\dot{\omega} - H_2u_p \end{aligned} \quad (14)$$

Here, H_2 defines the coupling matrix between flexible dynamics and piezoelectric actuators and u_p are the potential differences applied to the piezoelectric actuators and defined as [10],

$$u_p = H_2^T \begin{bmatrix} \Lambda_1 I & \Lambda_2 I \end{bmatrix} \begin{pmatrix} \eta \\ \psi \end{pmatrix} \quad (15)$$

By using Equation (13), dynamic of the flexible spacecraft may be obtained in first order form as [10],

$$\begin{aligned} \dot{\omega} &= J_{mb}^{-1} \left[H^T (C\psi + K\eta - CH\omega) + u \right] \\ \dot{\eta} &= \psi - H\omega \\ \dot{\psi} &= -(C\psi + K\eta - CH\omega) \end{aligned} \quad (16)$$

Defining, $J_{mb} = J - H^T H$ and $\psi = \dot{\eta} + H\omega$ is total velocity of the flexible beam. Then,

$$\begin{pmatrix} \dot{\eta} \\ \dot{\psi} \end{pmatrix} = A \begin{pmatrix} \eta \\ \psi \end{pmatrix} - ABH\omega \quad (17)$$

where, $A = \begin{pmatrix} 0 & I \\ -K & -C \end{pmatrix}$ and $B = \begin{pmatrix} 0 \\ I \end{pmatrix}$ with the appropriate dimensions. Also, equations of the flexible spacecraft with piezoelectric actuator may be obtained by using Equation (14),

$$\begin{aligned}\dot{\omega} &= J_{mb}^{-1} \left[H^T (C\psi + K\eta - CH\omega) + u + H^T H_2 u_p \right] \\ \dot{\eta} &= \psi - H\omega \\ \dot{\psi} &= -(C\psi + K\eta - CH\omega) - H_2 u_p\end{aligned}\quad (18)$$

For the sake of simplicity in developing control algorithm, Equation (18) may be written as,

$$\begin{aligned}\dot{\omega} &= J_{mb}^{-1} \left[H^T (C\psi + K\eta - CH\omega) + u + H^T H_2 u_p \right] \\ \begin{pmatrix} \dot{\eta} \\ \dot{\psi} \end{pmatrix} &= \bar{A} \begin{pmatrix} \eta \\ \psi \end{pmatrix} - ABH\omega\end{aligned}\quad (19)$$

Here, $\bar{A} = A - BH_2 H_2^T [\Lambda_1 I \quad \Lambda_2 I] = \begin{pmatrix} 0 & I \\ -(K + \Lambda_1 H_2 H_2^T) & -(C + \Lambda_2 H_2 H_2^T) \end{pmatrix}$, with the appropriate dimensions. Also, using the modal coordinates total vibration energy may be written as [10],

$$E_t = \dot{\eta}^T \dot{\eta} + \eta^T K \eta \quad (20)$$

3. Attitude Control Algorithms

In this section, Lyapunov function based feedback control algorithms are developed. In developing these algorithms two cases are considered. These cases are listed in **Table 1**. Both cases assume that body attitude and angular velocities are measured. In addition, a number of modal coordinates are also estimated from piezoelectric sensor measurements. On the other hand, the first case assumes only rigid body actuators such as reaction wheels are present. The second case assumes that there are a number of discrete piezoelectric patches that can affect the number of modes being controlled. In each case, one control algorithm is based on the classical *to-go* quaternion attitude propagation, while the other algorithm takes the derivative of the desired attitude (Equation (11)) into account.

Table 1: Control System Design

Case	Actuators	Sensors
I	Attitude Actuators	Attitude and Modal Sensors
II	Attitude and Piezo Actuators	Attitude and Modal Sensors

3.1 Case I: Attitude Control Actuators with Attitude and Modal Sensors

Two control objectives are sought for: track the desired attitude without a vibration in the satellite attitude and structure. Consequently, control law must ensure the spacecraft attitude tracks the desired attitude without excessive jitter. The second requirement is that the vibration of spacecraft's flexible appendages shall also be small.

Since, the *to-go* quaternion defines the difference between the desired attitude and realized attitude (i.e. attitude error), attitude tracking will be realized if the vectorial part of *to-go* attitude goes to zero: $\lim_{t \rightarrow \infty} \mathbf{t} = \mathbf{0}$ (or, $\lim_{t \rightarrow \infty} t_4 = 1$). To damp out vibrations in various modes, on the other hand, is realized if the vector of modal coordinates vector goes to zero: $\lim_{t \rightarrow \infty} \boldsymbol{\eta} = \mathbf{0}$.

3.1.1 Attitude Control Using *to-go* Quaternion

Theorem: The following controller brings the attitude to the desired one in a stable fashion:

$$\mathbf{u} = k_p \mathbf{t} - k_d \boldsymbol{\omega} - H^T (C\boldsymbol{\psi} + K\boldsymbol{\eta} - CH\boldsymbol{\omega}) \quad (21)$$

for $k_p > 0$ and $k_d > 0$ properly selected.

Proof: Consider the following positive definite Lyapunov function:

$$\begin{aligned} V &= V_1 + V_2 \\ V_1 &= 2(k_p)(1-t_4) + \frac{1}{2} \boldsymbol{\omega}^T J_{mb} \boldsymbol{\omega} \\ V_2 &= \frac{1}{2} (\boldsymbol{\eta}^T \quad \boldsymbol{\psi}^T) P_1 \begin{pmatrix} \boldsymbol{\eta} \\ \boldsymbol{\psi} \end{pmatrix} \end{aligned} \quad (22)$$

where $P_1 = P_1^T > 0$

Taking time derivative of Equation (22) to show asymptotic stability,

$$\begin{aligned} \dot{V}_1 &= -2(k_p)\dot{t}_4 + \boldsymbol{\omega}^T J_{mb} \dot{\boldsymbol{\omega}} \\ \dot{V}_2 &= (\boldsymbol{\eta}^T \quad \boldsymbol{\psi}^T) P_1 \begin{pmatrix} \dot{\boldsymbol{\eta}} \\ \dot{\boldsymbol{\psi}} \end{pmatrix} \end{aligned} \quad (23)$$

Substituting Equation (12), Equation (16) and Equation (21) into the Equation (23), and also substituting Equation (17) into the Equation (23),

$$\begin{aligned} \dot{V}_1 &= -\boldsymbol{\omega}^T k_d \boldsymbol{\omega}, \dot{V}_2 = (\boldsymbol{\eta}^T \quad \boldsymbol{\psi}^T) P_1 \left[A \begin{pmatrix} \boldsymbol{\eta} \\ \boldsymbol{\psi} \end{pmatrix} - ABH\boldsymbol{\omega} \right] \\ \dot{V}_2 &= (\boldsymbol{\eta}^T \quad \boldsymbol{\psi}^T) P_1 \left[A \begin{pmatrix} \boldsymbol{\eta} \\ \boldsymbol{\psi} \end{pmatrix} - ABH\boldsymbol{\omega} \right] \end{aligned} \quad (24)$$

Then,

$$\dot{V} = -\boldsymbol{\omega}^T k_d \boldsymbol{\omega} + (\boldsymbol{\eta}^T \quad \boldsymbol{\psi}^T) P_1 A \begin{pmatrix} \boldsymbol{\eta} \\ \boldsymbol{\psi} \end{pmatrix} - (\boldsymbol{\eta}^T \quad \boldsymbol{\psi}^T) P_1 A B H \boldsymbol{\omega} = \boldsymbol{x}^T Q_6 \boldsymbol{x} \leq 0 \quad (25)$$

where $\boldsymbol{x} = (\boldsymbol{\omega}^T \quad \boldsymbol{\eta}^T \quad \boldsymbol{\psi}^T)^T$ is the state vector and P_1 may be computed as the solution of the Lyapunov equation as before, and,

$$\begin{aligned} Q_6 &= \begin{pmatrix} -k_d I & -Q_3^T \\ -Q_3 & -Q_1 \end{pmatrix} \\ -Q_1 &= \frac{1}{2} [P_1 A + A^T P_1] \\ Q_3 &= \frac{P_1 A B H}{2} \end{aligned} \quad (26)$$

Note that Lyapunov stability theorem indicates that given a stable matrix, A , and a positive definite matrix P , can be found such that $-Q = PA + A^T P$ where Q is also positive definite [11]. Using the Lyapunov stability theorem, the matrix Q_1 is a fixed positive definite matrix and solution of the P_1 exists because $\sigma(A) \subset \mathbb{C}^-$, with $\sigma(\cdot)$ denoting the set of eigenvalues. Then, the matrix Q_6 is negative definite, $\sigma(Q_6) \subset \mathbb{C}^-$, for properly selected k_d .

3.1.2 Attitude Control Using *to-go* Quaternion with the Derivative of the Desired Attitude

To-go attitude propagation algorithm presented Equation (11) is employed in this section. It offers a more precise trajectory tracking solution since derivative of the desired trajectory is taken into account.

Theorem: The following controller brings the attitude to the desired one in a stable fashion:

$$\boldsymbol{u} = k_p \boldsymbol{t} - k_d \boldsymbol{\omega} + 2(k_d \boldsymbol{s} + J_{mb} \dot{\boldsymbol{s}}) - H^T (C\boldsymbol{\psi} + K\boldsymbol{\eta} - CH\boldsymbol{\omega}) \quad (27)$$

for all $k_p > 0$ and $k_d > 0$ properly selected.

Proof: Consider the positive definite Lyapunov function:

$$\begin{aligned} V &= V_3 + V_2 \\ V_3 &= 2k_p(1-t_4) + \frac{1}{2}(-2\boldsymbol{s} + \boldsymbol{\omega})^T J_{mb}(-2\boldsymbol{s} + \boldsymbol{\omega}) \\ V_2 &= \frac{1}{2}(\boldsymbol{\eta}^T \quad \boldsymbol{\psi}^T) P_1 \begin{pmatrix} \boldsymbol{\eta} \\ \boldsymbol{\psi} \end{pmatrix} \end{aligned} \quad (28)$$

where $P_1 = P_1^T > 0$

Taking time derivative of Equation (28) to show asymptotic stability,

$$\begin{aligned}\dot{V}_3 &= -2(k_p)\dot{t}_4 + (-2s + \omega)^T J_{mb}(-2\dot{s} + \dot{\omega}) \\ \dot{V}_2 &= (\eta^T \quad \psi^T)P_1 \begin{pmatrix} \dot{\eta} \\ \dot{\psi} \end{pmatrix}\end{aligned}\quad (29)$$

Substituting Equation (11), Equation (16) and Equation (27) into the Equation (29), and substituting Equation (17) into the Equation (29),

$$\begin{aligned}\dot{V}_3 &= -(-2s + \omega)^T k_d(-2s + \omega) \\ \dot{V}_2 &= (\eta^T \quad \psi^T)P_1 \left[A \begin{pmatrix} \eta \\ \psi \end{pmatrix} - ABH\omega \right]\end{aligned}\quad (30)$$

Then,

$$\begin{aligned}\dot{V} &= -(-2s + \omega)^T k_d(-2s + \omega) + (\eta^T \quad \psi^T)P_1 A \begin{pmatrix} \eta \\ \psi \end{pmatrix} - (\eta^T \quad \psi^T)P_1 ABH\omega \\ \dot{V} &= -(2s)^T k_d(2s) + x^T Q_6 x\end{aligned}\quad (31)$$

where $x = (\omega^T \quad \eta^T \quad \psi^T)^T$ is state vector with

$$\begin{aligned}Q_6 &= \begin{pmatrix} -k_d I & -Q_3^T \\ -Q_3 & -Q_1 \end{pmatrix} \\ -Q_1 &= \frac{1}{2} [P_1 A + A^T P_1] \\ Q_3 &= \frac{P_1 ABH}{2}\end{aligned}\quad (32)$$

Using the Lyapunov stability theorem [11], the matrix Q_1 is a fixed positive definite matrix with the P_1 is the solution of Sylvester equation and exists because $\sigma(\bar{A}) \subset \mathbb{C}^-$, with $\sigma(\cdot)$ denoting the set of eigenvalues. Then, the matrix Q_6 is also negative definite, $\sigma(Q_6) \subset \mathbb{C}^-$, for properly selected k_d .

Consequently, the proposed controller (Equation (27)), brings the system to the desired attitude asymptotically.

3.2 Case II: Attitude and Piezoelectric Actuators with Attitude and Modal Sensors

In this section, in addition to attitude control actuators, piezoelectric actuators to damp out structural vibrations are added employed in the feedback control system.

3.2.1 Attitude Control Using *to-go* Quaternion

Theorem: The following controller brings the attitude to the desired one in a stable fashion:

$$u = k_p \mathbf{t} - k_d \boldsymbol{\omega} - H^T (C\boldsymbol{\psi} + K\boldsymbol{\eta} - CH\boldsymbol{\omega}) - H^T H_2 u_p \quad (33)$$

for $k_p > 0$ and $k_d > 0$ properly selected.

Proof: Given control law may be derived using a properly selected Lyapunov function. Consider the following positive definite Lyapunov function:

$$\begin{aligned} V &= V_1 + V_2 \\ V_1 &= 2(k_p)(1-t_4) + \frac{1}{2} \boldsymbol{\omega}^T J_{mb} \boldsymbol{\omega} \\ V_2 &= \frac{1}{2} (\boldsymbol{\eta}^T \quad \boldsymbol{\psi}^T) P_2 \begin{pmatrix} \boldsymbol{\eta} \\ \boldsymbol{\psi} \end{pmatrix} \end{aligned} \quad (34)$$

where $P_2 = P_2^T > 0$

Taking time derivative of Equation (34) to show asymptotic stability,

$$\begin{aligned} \dot{V}_1 &= -2(k_p)\dot{t}_4 + \boldsymbol{\omega}^T J_{mb} \dot{\boldsymbol{\omega}} \\ \dot{V}_2 &= (\boldsymbol{\eta}^T \quad \boldsymbol{\psi}^T) P_2 \begin{pmatrix} \dot{\boldsymbol{\eta}} \\ \dot{\boldsymbol{\psi}} \end{pmatrix} \end{aligned} \quad (35)$$

Substituting Equation (12), Equation (19) and Equation (33) into the Equation (35),

$$\begin{aligned} \dot{V}_1 &= -\boldsymbol{\omega}^T k_d \boldsymbol{\omega} \\ \dot{V}_2 &= (\boldsymbol{\eta}^T \quad \boldsymbol{\psi}^T) P_2 \left[\bar{A} \begin{pmatrix} \boldsymbol{\eta} \\ \boldsymbol{\psi} \end{pmatrix} - ABH\boldsymbol{\omega} \right] \end{aligned} \quad (36)$$

Then,

$$\dot{V} = -\boldsymbol{\omega}^T k_d \boldsymbol{\omega} + (\boldsymbol{\eta}^T \quad \boldsymbol{\psi}^T) P_2 \bar{A} \begin{pmatrix} \boldsymbol{\eta} \\ \boldsymbol{\psi} \end{pmatrix} - (\boldsymbol{\eta}^T \quad \boldsymbol{\psi}^T) P_2 ABH\boldsymbol{\omega} = \mathbf{x}^T Q_7 \mathbf{x} \leq 0 \quad (37)$$

where $\mathbf{x} = (\boldsymbol{\omega}^T \quad \boldsymbol{\eta}^T \quad \boldsymbol{\psi}^T)^T$ is the state vector

$$\begin{aligned} Q_7 &= \begin{pmatrix} -k_d I & -Q_4^T \\ -Q_4 & -Q_2 \end{pmatrix} \\ -Q_2 &= \frac{1}{2} [P_2 \bar{A} + \bar{A}^T P_2] \\ Q_4 &= \frac{P_2 ABH}{2} \end{aligned} \quad (38)$$

Using the Lyapunov stability theorem [11], the matrix Q_2 is a fixed positive definite matrix and solution of the P_2 exists because $\sigma(\bar{A}) \subset \mathbb{C}^-$, with $\sigma(\cdot)$ denoting the set of eigenvalues. Then, the matrix Q_7 is negative definite, $\sigma(Q_7) \subset \mathbb{C}^-$, for properly selected k_d , proving asymptotic stability of the proposed controller.

3.2.2 Attitude Control Using *to-go* Quaternion with the Derivative of the Desired Attitude

Again the *to-go* attitude propagation algorithm given in Equation (11) is used in this section.

Theorem: The following controller brings the attitude to the desired one in a stable fashion:

$$u = k_p \mathbf{t} - k_d \boldsymbol{\omega} + 2(k_d \mathbf{s} + J_{mb} \dot{\mathbf{s}}) - H^T (C\boldsymbol{\psi} + K\boldsymbol{\eta} - CH\boldsymbol{\omega}) - H^T H_2 u_p \quad (39)$$

for all $k_p > 0$ and $k_d > 0$ properly selected.

Proof: Given control law may be derived using a properly selected Lyapunov function. Positive definite Lyapunov function:

$$\begin{aligned} V &= V_3 + V_2 \\ V_3 &= 2k_p(1-t_4) + \frac{1}{2}(-2\mathbf{s} + \boldsymbol{\omega})^T J_{mb}(-2\mathbf{s} + \boldsymbol{\omega}) \\ V_2 &= \frac{1}{2}(\boldsymbol{\eta}^T \quad \boldsymbol{\psi}^T) P_2 \begin{pmatrix} \boldsymbol{\eta} \\ \boldsymbol{\psi} \end{pmatrix} \end{aligned} \quad (40)$$

where $P_2 = P_2^T > 0$

Taking time derivative of Equation (40) to show asymptotic stability,

$$\begin{aligned} \dot{V}_3 &= -2(k_p)\dot{t}_4 + (-2\mathbf{s} + \boldsymbol{\omega})^T J_{mb}(-2\dot{\mathbf{s}} + \dot{\boldsymbol{\omega}}) \\ \dot{V}_2 &= (\boldsymbol{\eta}^T \quad \boldsymbol{\psi}^T) P_2 \begin{pmatrix} \dot{\boldsymbol{\eta}} \\ \dot{\boldsymbol{\psi}} \end{pmatrix} \end{aligned} \quad (41)$$

Substituting Equation (11), Equation (19) and Equation (39) into the Equation (41),

$$\begin{aligned} \dot{V}_3 &= -(-2\mathbf{s} + \boldsymbol{\omega})^T k_d(-2\mathbf{s} + \boldsymbol{\omega}) \\ \dot{V}_2 &= (\boldsymbol{\eta}^T \quad \boldsymbol{\psi}^T) P_2 \left[\bar{A} \begin{pmatrix} \boldsymbol{\eta} \\ \boldsymbol{\psi} \end{pmatrix} - ABH\boldsymbol{\omega} \right] \end{aligned} \quad (42)$$

Then,

$$\begin{aligned} \dot{V} &= -(-2\mathbf{s} + \boldsymbol{\omega})^T k_d(-2\mathbf{s} + \boldsymbol{\omega}) + (\boldsymbol{\eta}^T \quad \boldsymbol{\psi}^T) P_2 \bar{A} \begin{pmatrix} \boldsymbol{\eta} \\ \boldsymbol{\psi} \end{pmatrix} - (\boldsymbol{\eta}^T \quad \boldsymbol{\psi}^T) P_2 ABH\boldsymbol{\omega} \\ \dot{V} &= -(2\mathbf{s})^T k_d(2\mathbf{s}) + \mathbf{x}^T Q_7 \mathbf{x} \end{aligned} \quad (43)$$

where $\mathbf{x} = (\boldsymbol{\omega}^T \quad \boldsymbol{\eta}^T \quad \boldsymbol{\psi}^T)^T$ is state vector with

$$\begin{aligned}
Q_7 &= \begin{pmatrix} -k_d I & -Q_4^T \\ -Q_4 & -Q_2 \end{pmatrix} \\
-Q_2 &= \frac{1}{2} [P_2 \bar{A} + \bar{A}^T P_2] \\
Q_4 &= \frac{P_2 ABH}{2}
\end{aligned} \tag{44}$$

Using the Lyapunov stability theorem [11], once the matrix Q_2 is a fixed positive definite matrix with the P_1 is the solution of Sylvester equation and exists because $\sigma(\bar{A}) \subset \mathbb{C}^-$, with $\sigma(\cdot)$ denoting the set of eigenvalues. Then, the matrix Q_7 is negative definite, $\sigma(Q_7) \subset \mathbb{C}^-$, for properly selected k_d . As it derived in Section (4.3.1), we may find that the largest invariant set \mathcal{E} with the help of LaSalle theorem. Then all the control objectives are satisfied.

4. Simulation Results and Discussion

Simulation of the mathematical model of the flexible spacecraft attitude dynamics is developed in MATLAB/Simulink environment. The desired attitude is defined as a time dependent function. A Cubic function is taken for the rotation angle. By using initial and final conditions, rotation angle coefficients may be obtained. Simulation time is selected as 100 seconds. Simulation parameters for the attitude are given in Table 2.

Table 2: Simulation Parameters for Attitude Dynamic

Parameter	Value
Desired Attitude	$\begin{Bmatrix} \mathbf{d} \\ d_4 \end{Bmatrix} = \begin{Bmatrix} \lambda \sin(\alpha / 2) \\ \cos(\alpha / 2) \end{Bmatrix}$
Prescribe Time Dependent Rotation Angle	$\alpha = a + bt + ct^2 + et^3$
Initial and Final Values of the Rotation Angles and their Derivatives	$\alpha_0 = 0 \quad \dot{\alpha}_0 = 0 \quad \alpha_f = \frac{2\pi}{3} \quad \dot{\alpha}_f = 0$
Eigen Axis of the Rotation	$\lambda = (1, 2, 3)^T / \sqrt{14}$
Duration of Rotation	$t_f = 100 \text{ s}$

In the simulations, the flexible spacecraft is assumed to have only four bending modes. In Table 3, natural frequency and damping ratio of the related modes are given [12].

Table 3: Parameters of Flexible Spacecraft

	Natural Frequency(rad/s)	Damping Ratio
Mode 1	0.7681	0.005607
Mode 2	1.1038	0.00862
Mode 3	1.8733	0.01283
Mode 4	2.5496	0.02516

The characteristics of the piezoelectric are specified by the piezoelectric charge constant, c , the Young modulus of elasticity E_p , and the thickness b_p , are listed in Table 4 along with the bounding layer parameters. The length, width and thickness of the flexible panel are, l , l_a and l_b , respectively. The bending moment M_p due to piezoelectric films is proportional to the applied voltage according to $M_p = -c u_p$ with [10]

$$c = c_p l_a E_p \frac{E_b b_b (b_p + b_b) + E l_b (b_p + 2b_b + l_b)}{2(E_p b_p + E_b b_b + E l_b)} Nm/V \quad (45)$$

Table 4: Characteristics of the Piezoelectric Material and Bonding Layer, and of the Flexible Panel

Piezoelectric Layer	Flexible Panel
$c_p = 171 \times 10^{-12} \text{ m}$	$l = 5 \text{ m}$
$E_p = 139 \times 10^9 \text{ N/m}^2$	$l_a = 0.8 \text{ m}$
$b_p = 2.1 \times 10^{-3} \text{ m}$	$l_b = 0.1 \text{ m}$
	$E = 6.8 \times 10^{10} \text{ N/m}^2$

Rigid body inertia matrix, coupling matrices and controller parameters are also given in Table 5 [12]. The feedback gains, $k_p = 1000$, $k_d = 1000$.

Table 5: Simulation Parameters used for the Controller and the Flexible Spacecraft Model

Parameter	Value
Control Parameters	$k_p = 1000, k_d = 1000$
Piezoelectric Actuator Control Parameters	$\Lambda_1 = 100, \Lambda_2 = 100$
Rigid Body Moment of Inertia	$J_{mb} = \begin{bmatrix} 350 & 3 & 4 \\ 3 & 280 & 10 \\ 4 & 10 & 190 \end{bmatrix} \text{ kgm}^2$
Coupling Matrix between Flexible and Rigid Dynamics	$H = \begin{bmatrix} 6.45637 & 1.27814 & 2.15629 \\ -1.25619 & 0.91756 & -1.67264 \\ 1.11687 & 2.48901 & -0.83674 \\ 1.23637 & -2.6581 & -1.12503 \end{bmatrix} \sqrt{\text{kgm/s}^2}$
Coupling Matrix between Flexible Dynamics and the Three Piezoelectric Actuators	$H_2 = \begin{bmatrix} 2.3425 \times 10^{-2} \\ -4.2253 \times 10^{-3} \\ 3.9129 \times 10^{-2} \\ 7.0261 \times 10^{-2} \end{bmatrix} \sqrt{\text{kgm/Vs}^2}$

On the other hand, when piezoelectric actuators are present and chosen as shown in Table 5, they increase the stiffness and the internal damping of the system. Piezoelectric actuators' feedback gain values, Λ_1 , Λ_2 are selected so that eigenvalues of the dynamics of the bending modes have natural frequencies $\omega_0 = [0.7988 \ 1.1045 \ 1.9078 \ 2.6497]^T$ while for damping $\zeta_0 = [0.009 \ 0.012 \ 0.018 \ 0.152]^T$, are achieved.

4.1 Rigid Body Simulation Results

The simulations are carried out first to show the effectiveness of the tracking controller where the desired attitude and its derivative are taken into account. Thus, the flexible modes are not included in the simulation model. The results of the tracking controller is compared with those of the classical quaternion feedback controller. In Figure 1, component wise difference between desired and realized attitude for classical attitude controller is given. Same graph for tracking attitude controller can be seen in Figure 2. Comparing Figure 1 and Figure 2, it may easily be observed that tracking controller tracks the desired trajectory about two orders of magnitude better than the classical controller.

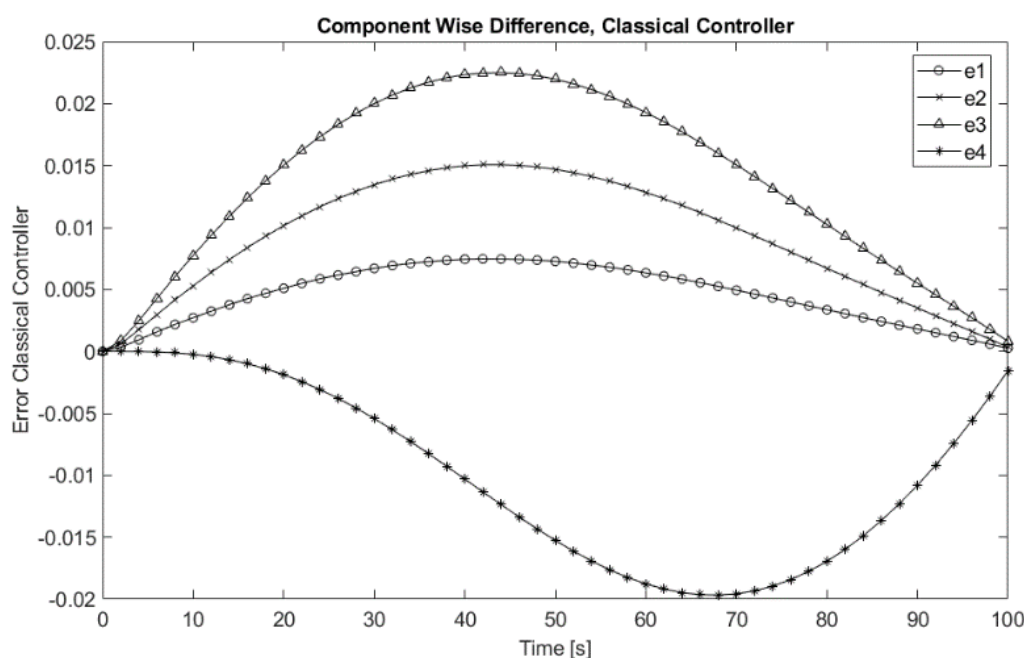


Figure 1: Component Wise Difference between Desired and Realized Quaternion with Classical Controller (no structural modes)

4.2 Simulation Results for Case I

In this section, results of the simulations carried out by assuming that only attitude control actuators are present in the system. The controller utilizes attitude, angular velocity and modal coordinates measured. In Section 3.1, the associated formulation was given. First classical attitude control of Section 3.1.1 is simulated. To understand the effect on structural modes, the vibration energy (Equation (20)) of the spacecraft is plotted in Figure 3.

Using the tracking controller given in Section 3.1.2, the vibration energy graph is also obtained and presented in Figure 4. Both controllers required similar amounts of control torque. However, as it may be observed from the figures, with tracking controller the total vibration energy is decreased by about 20% as compared to the classical controller. The simulation results show that the success of tracking algorithm to suppress the vibration effects on the spacecraft while using almost the same amount of control torque.

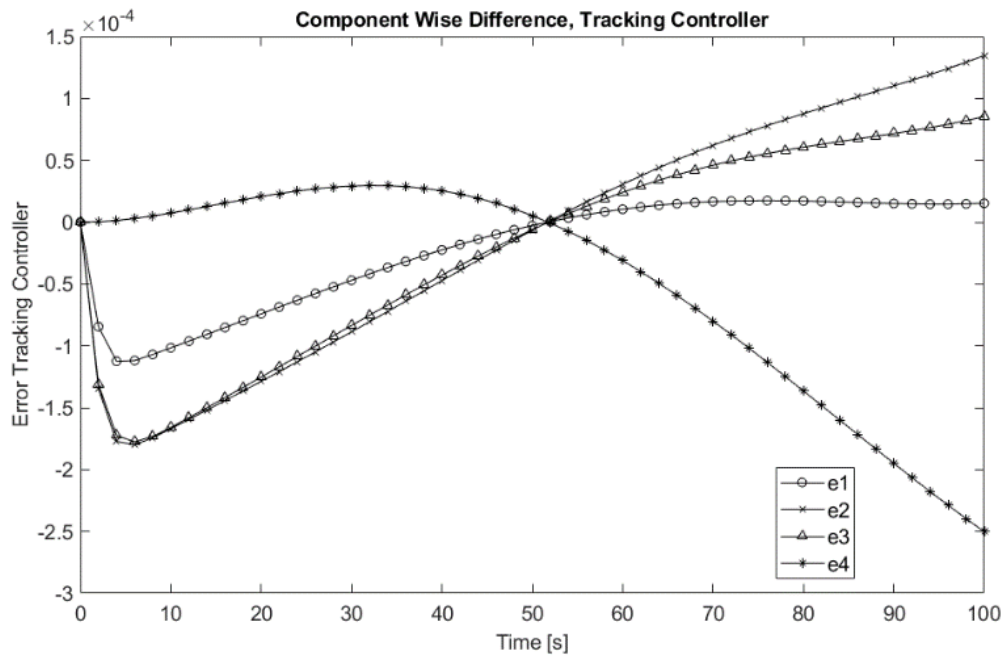


Figure 2: Component Wise Difference between Desired and Realized Quaternion with Tracking Attitude Controller (no structural modes)

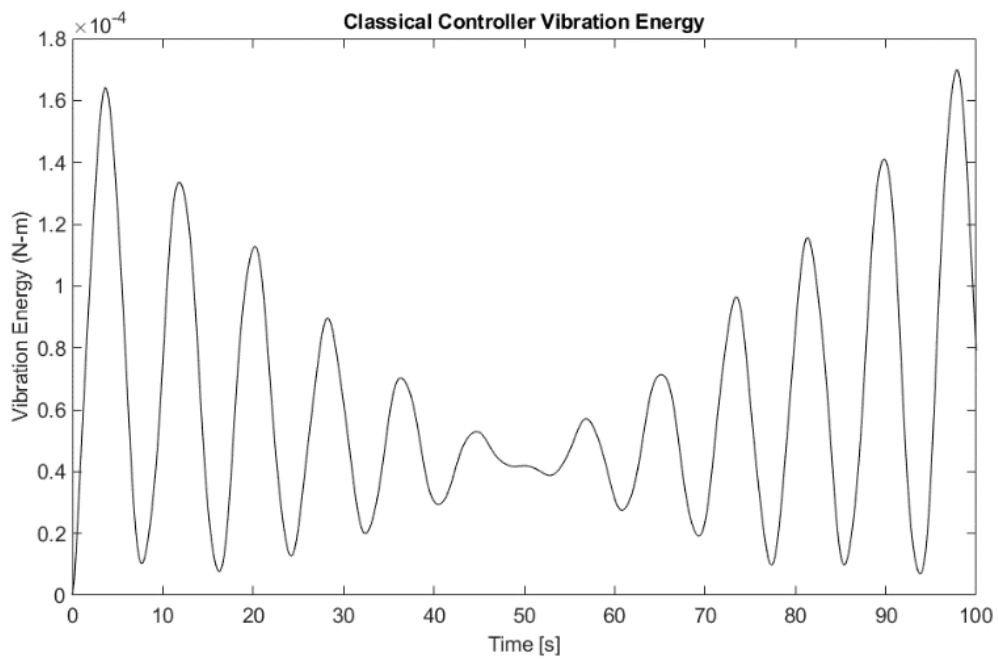


Figure 3: Time history of the Vibration Energy with Classical Controller

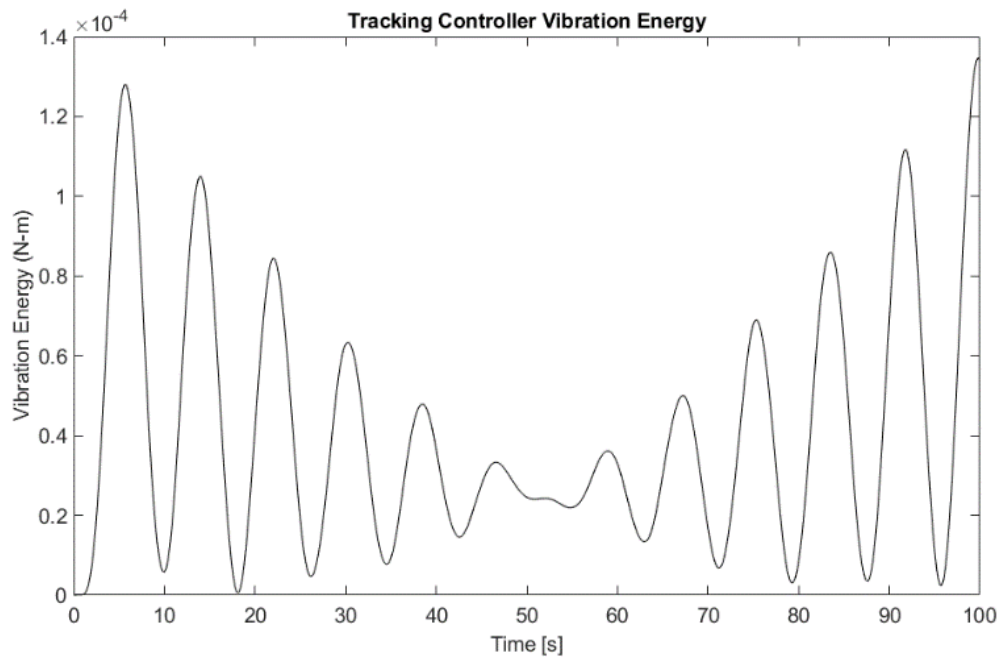


Figure 4: Time history of the Vibration Energy with Tracking Controller

4.3 Simulation results for Case II

In this section, simulation is performed by adding piezoelectric actuators to the system. Using the controller in Section 3.2.1, the generated vibration energy is obtained and presented in Figure 5. The control torque created by piezoelectric actuators may also be observed from Figure 6. Comparing Figure 5 with Figure 3, it may be observed that vibration energy on the spacecraft system is decreased considerably and damped out much faster with the utilization of piezoelectric actuators. The actuator voltages are also quite small.

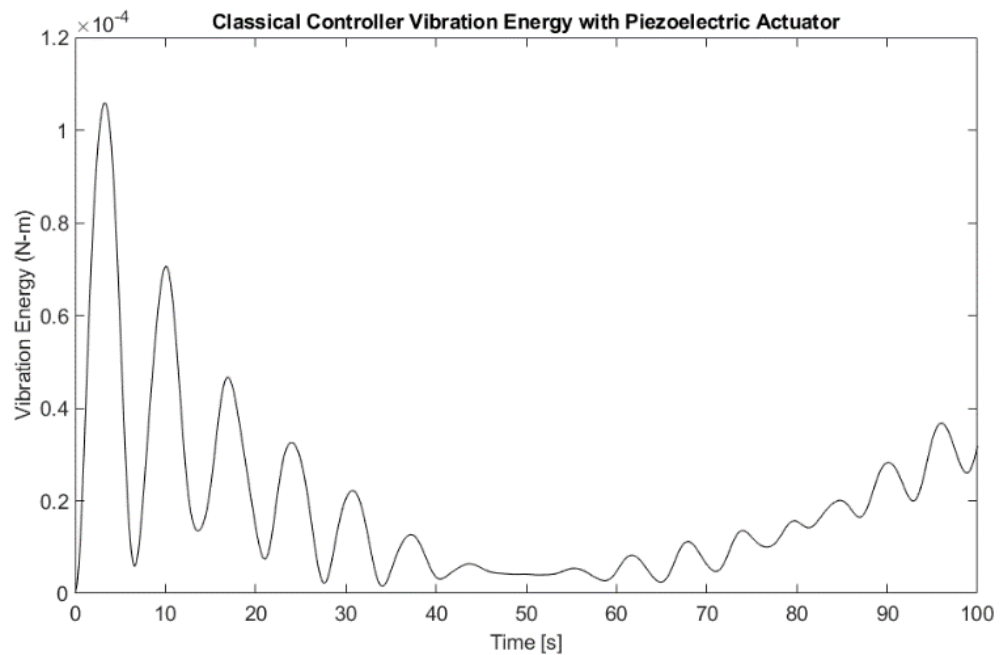


Figure 5: Time History of Classical Controller Vibration Energy with Piezoelectric Actuator

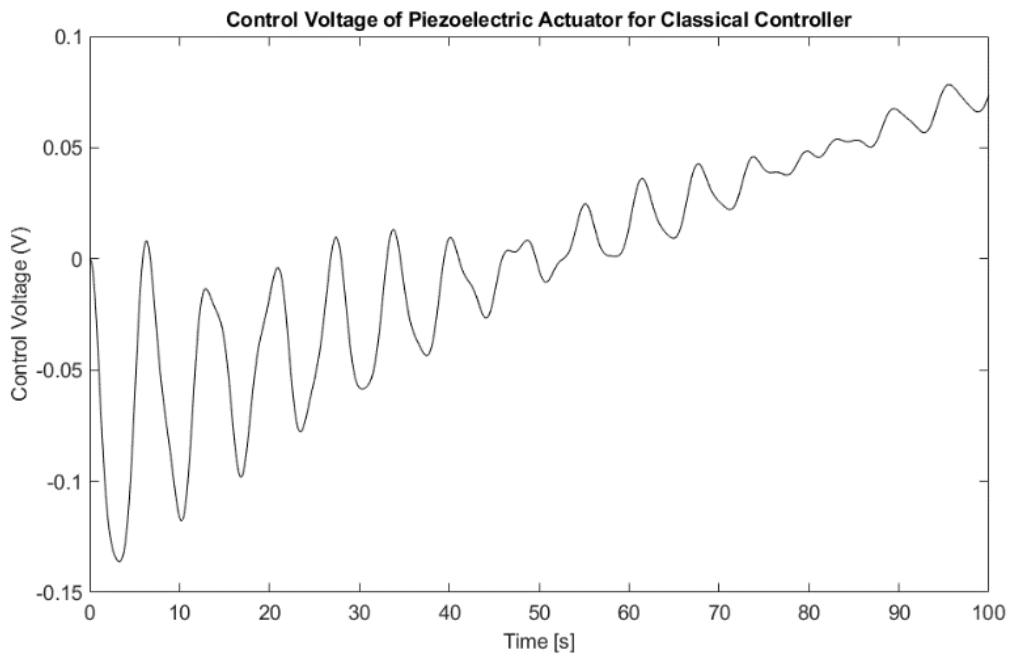


Figure 6: Time history of Control Voltage of the Middle Piezoelectric Actuator for Classical Controller

Simulation is repeated this time with the tracking controller of Section 3.2.2. The vibration energy history of the system is presented in Figure 7. The graph shows that with piezoelectric actuators and tracking controller, vibration energy is reduced by about 40%. Thus, the best solution for the vibration problem is obtained using tracking attitude controller together with the piezoelectric actuators. Moreover, as it may be observed from Figure 8 that tracking controller needs lower control effort on piezoelectric actuators.

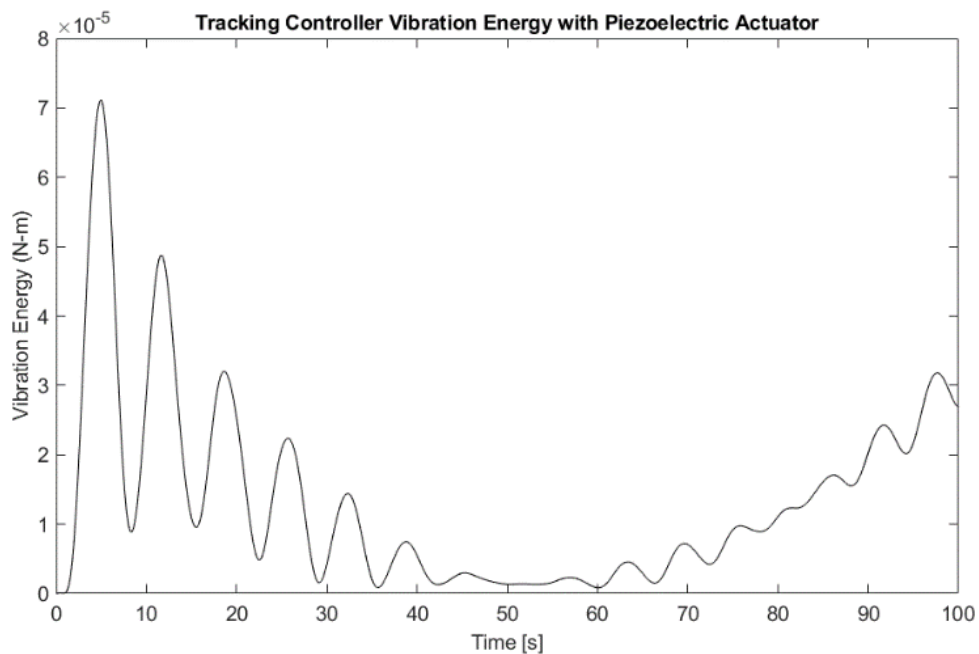


Figure 7: Time History of Tracking Controller Vibration Energy with Piezoelectric Actuator

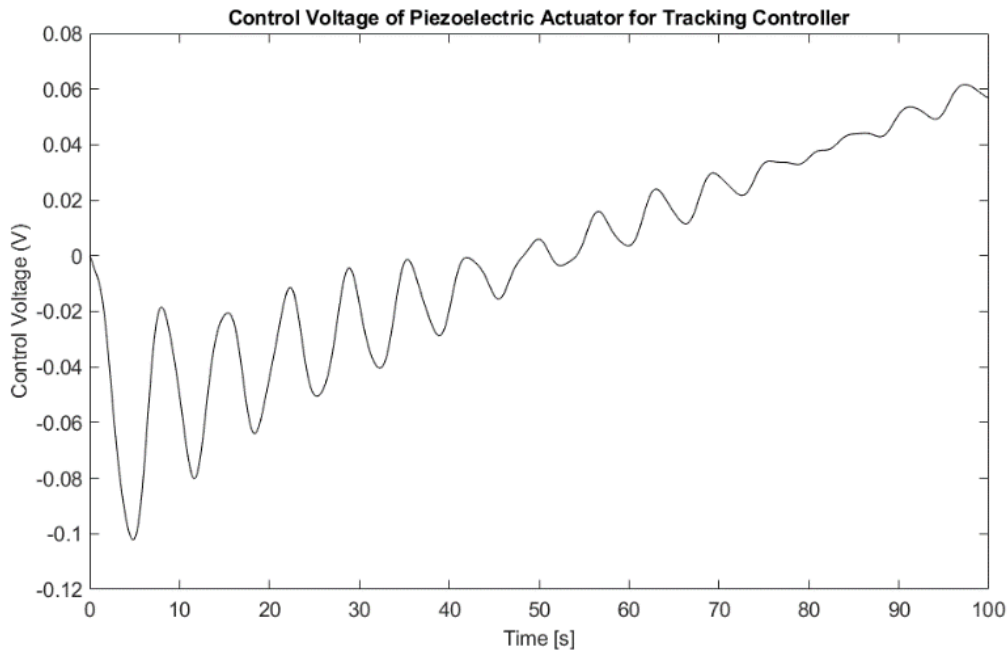


Figure 8: Time History of Control Voltage of the Middle Piezoelectric Actuator for Tracking Controller

5. Conclusions

New attitude control algorithms for the slew maneuver of flexible satellites is presented. It is shown that the tracking control achieves much higher pointing accuracy. With flexible modes included, the vibration energy of the tracking controller is much lower than that achieved with the classical controller. Including piezoelectric actuators, help damp out vibration much faster. In this case tracking controller also outperforms the classical controller.

In all cases, the success of the tracking controllers developed is demonstrated through simulations for missions when high pointing performance and low vibration energy is required.

References

- [1] Vago, J., Gardini, B., Baglioni, P., Kminek, G., Gianfiglio, G., & Project Team, "Science objectives of ESA's ExoMars mission," 2018.
- [2] Baz, A., and Poh, S., "Performance of an Active Control System with Piezoelectric Actuators," *Journal of Sound and Vibration*, vol. 126, no. 2, pp. 327-343, 1988.
- [3] Li, Z., and Bainum, P. M., "Vibration Control of Flexible Spacecraft Integrating a Momentum Exchange Controller and a Distributed Piezoelectric Actuator," *Journal of Sound and Vibration*, vol. 177, no. 4, pp. 539-553, 1994.
- [4] Hyland, D. C., Junkins, J. L., and Longman, R. W., "Active Control Technology for Large Space Structures," *Journal of Guidance, Control, and Dynamics*, vol. 16, no. 5, pp. 801-821, 1993.
- [5] Crawley, E. F., and De Luis, J., "Use of Piezoelectric Actuators as Elements of Intelligent Structures," *AIAA Journal*, vol. 25, no. 10, pp. 1373-1385, 1987.
- [6] Yang, S. M., and Lee, Y. J. "Modal Analysis of Stepped Beams with Piezoelectric Materials," *Journal of Sound and Vibration*, vol. 176, no. 3, pp. 289-300, 1994.
- [7] Wie, B., *Space Vehicle Dynamics and Control*, AIAA Inc., 2nd ed., 2008.
- [8] Tekinalp, O., Gomroki, M. M., and Ataş, O., "Nonlinear Tracking Attitude Control of Spacecraft on Time Dependent Trajectories," *AAS/AIAA Astrodynamics Specialist Conference*, Vail, CO, August 9-13, 2015.
- [9] Tekinalp, O., and Tekinalp, A., "Tracking Control of Spacecraft Attitude on Time Dependent Trajectories," *AIAA/AAS Astrodynamics Specialist Conference*, Long Beach, CA, September 13-16, 2016.

- [10] Gennaro, S., "Output Stabilization of Flexible Spacecraft with Active Vibration Suppression," IEEE Transactions on Aerospace and Electronic Systems, vol. 39, no. 3, pp. 747-759, 2003.
- [11] Khalil, H. K., "Nonlinear Systems," New Jersey: Upper Saddle River, 1996.
- [12] Hu, Q., "Robust Adaptive Sliding Mode Attitude Control and Vibration Damping of Flexible Spacecraft Subject to Unknown Disturbance and Uncertainty," Transactions of the Institute of Measurement and Control, vol. 34, no. 4, pp. 436-447, 2011.